

4 EXPERIMENTAL FACILITIES IN BEAM HALL

4.1 SCATTERING CHAMBER AND NEUTRON ARRAY

N. Saneesh, K. S. Golda, Mohit Kumar, A. Jhingan and P. Sugathan

4.1.1 Maintenance and servicing activities of GPSC (with technical / engineering support from the Vacuum Laboratory)

Low flux irradiation facility in the General Purpose Scattering Chamber (GPSC) was used by the ISRO group for pre-launch radiation hardness testing of electronic devices. A couple of such experiments were carried out by ISRO laboratories and one nuclear physics experiment was performed using the GPSC facility in the last year.

The signal processing electronics and data acquisition system for the GPSC experiments had been installed in the Data Room which was quite far away from the experimental hall. With ageing and contamination in the contacts, the quality of signals transmitted to the signal processing electronics deteriorated over time. It was noticed that the time and energy resolutions were being compromised in long distance transmission using the existing system. A new data acquisition system was recently commissioned locally in the GDA cabin. All the co-axial cables used for signal transmission were re-routed and tested for this purpose. Even though the cables were old, the length became much shorter for the local data acquisition system which effectively improved the signal quality.

4.1.2 Maintenance and servicing activities of NAND (with technical / engineering support from Vacuum, Beam Transport and Electronics Laboratories)

The Photo-Multiplier Tubes (PMTs) coupled to the neutron detectors are biased by both imported and home-made multi-channel high voltage power supplies. The power supplies are kept near the detectors in the beam hall which has an ambience of high dust level. Therefore, cleaning and servicing of the power supplies are carried out at regular intervals for ensuring smooth functioning of the same. Individual power supplies were tested with appropriate input load to ensure their satisfactory performance before using them for biasing the PMTs. The zero-offset values for individual supplies were brought to zero or close to zero after completing the servicing.

The home-made signal processing electronics units including the Pulse Shape Discriminator (PSD) were also subjected to routine cleaning and maintenance. In order to ensure the best performance of the signal processing electronics, all the NIM bins, cooling fans etc. were also thoroughly cleaned with compressed air after dismantling them from their respective spaces. All the input and output signal connections of the electronic modules were restored after the maintenance.

The NAND target chamber requires two turbo-molecular pumps connected at the beam entrance and the exit ports to get the required vacuum with large area MWPCs in operation. The pump connected at the beam entrance side of the chamber was replaced by a newly procured turbo-molecular pump (pumping speed ~700 lps). The complete vacuum testing of the chamber was carried out after its installation. An ultimate pressure of $\sim 3 \times 10^{-6}$ mbar was achieved after pumping the chamber overnight.

4.1.3 Experiments using GPSC and NAND

The following experiments were carried out in GPSC using the Pelletron beam during last one year.

User / Affiliation	Experiment	Beam	No of shifts
Mr. Harun Al Rashid, Gauhati University, Assam.	Investigation of multi-nucleon transfer reactions and neutron-proton correlation: Effects of nuclear deformation and orientation.	^{10}B , ^{16}O	20
Dr. Harishanker Gupta ISRO, Balgalore	Single Event	^{30}Si , ^{12}C , ^{48}Ti , ^{58}Ni , ^{107}Ag , ^{197}Au	6
Dr. B. K. Sapra ISRO, Balgalore	Irradiation of passive dosimeters to Ion beams for Gaganyaan pre-mission studies	^7Li	9

4.1.4 Installation of local Data Acquisition System for GPSC (with technical / engineering support from the Data Support Laboratory)

A dedicated VME-based data acquisition (DAQ) system was installed for the GPSC facility in the GDA cabin. The existing signal cables from the GPSC-GDA beam lines were re-routed accordingly. The new data acquisition system consisted of home-made VME crate controller with commercial modules like ADC, TDC and QDC.

A thorough testing of the newly procured 16-channel multi event Charge to Digital Converter (QDC), V792N of CAEN, was carried out by making necessary modifications in the crate controller. A Time of Flight (ToF) consisting of two BaF₂ detectors was used for this purpose. A sealed ⁶⁰Co g-source was used in this set-up. One of the detectors was placed close to the source and the other at a distance of 30 cm on the opposite side of the source. The dynode signal from the detector placed close to the source was routed through a charge-sensitive pre-amplifier to a shaping amplifier with 0.5 ms shaping time. The amplifier output was digitized by an ADC to get the energy information. The anode signal from the close detector was split into two signals through a fast amplifier. One of the outputs of the fast-amplifier was fed to a CFD for generating a logic output. One of this logical output was delayed and used as the stop to the TDC and another output was delayed and stretched to a width of 500 ns to use as the gate for the QDC. The second output from the fast-amplifier was fed to the QDC for integrating the charge to get the energy information. The anode signal from the detector kept at a distance from the source was fed through a CFD to generate a logical output which was used as the master strobe for the DAQ, as well as the common start for the TDC. A TDC range of 200 ns was employed for this measurement. Figure 4.1.1 compares the energy of g-rays emitted by ⁶⁰Co recorded through conventional method of using spectroscopy amplifier output being digitized through an ADC and the integration of the charge through a QDC.

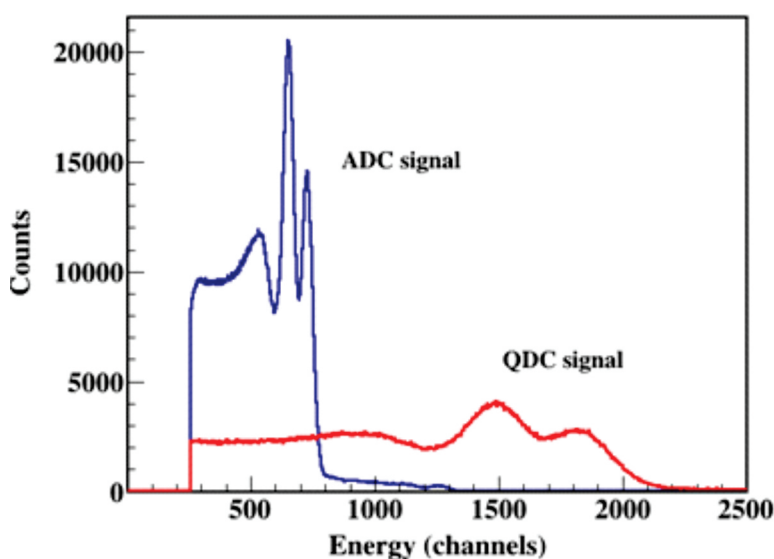


Fig. 4.1.1: The energy of g-rays emitted by ⁶⁰Co recorded through the conventional method compared with the charge integration method.

4.1.5 Performance evaluation of Pulse Shape Discrimination module with modified TOF circuit (with technical/ engineering support from the Electronics Laboratory)

In the earlier electronic design of the Pulse Shape Discrimination (PSD) module, the delayed CFD signal (called as ToF output) generation was contaminated due to high time jitter. Therefore, in any ToF measurement with respect to a reference detector, the time resolution was found to be inferior, ~ 2.8 ns, if ToF output was used as the stop signal. Whereas the measurements using prompt CFD output yielded ~ 1.0 ns time resolution. In the neutron ToF experiments, the time resolution is desired to be as minimum as possible since it is used for deriving the energy of neutrons. In order to minimize the time jitter, the ToF circuit was modified. The modified modules were tested first with a pulse generator and then with standard radioactive sources. The measurement set-up consisted of a BaF₂ detector as the reference and four BC501A detectors of the NAND array for ToF measurements. The path length for the ToF measurement was ~ 80 cm. A radioactive source, ⁶⁰Co, which emits minimum two g-rays per event was placed close to the BaF₂ detector. Commercial modules, Phillips Scientific 715 and Gate and Delay Generator (GDG) were used for processing the signal from the BaF₂ detector. The BC501A detector signals were processed using the modified PSD modules. A VME-based data acquisition system was used for recording the processed signals which included a light output signal, a zero-cross signal and a ToF signal from each neutron detector (total 12 parameters). The TDC range was set to be 200 ns and the corresponding channel resolution was 0.0494 ns/channel. The test results showed that the modification improved the time resolution to ~ 1 ns when ToF output had been used for the measurements. During the measurements, an unusual tailing was observed in some of the spectra. These errors were fixed and the modules were tested again for the stability in performance. The histogram showing the width obtained when ~ 50 modules were tested is given in Figure 4.1.2.

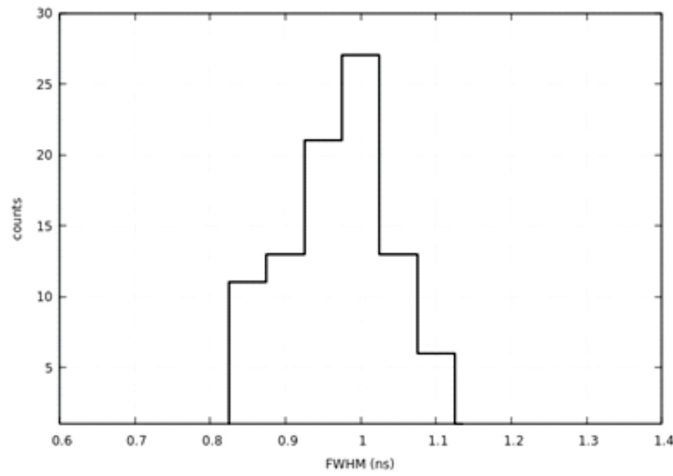


Fig. 4.1.2: Histogram shows the width obtained when ~ 50 modules were tested.

4.1.6 Energy measurement of neutrons from Am-Be source

A. T. Fathima Shirin Shana¹, Divya Arora² and NAND group

¹Department of Physics, Government Arts and Science College, Calicut 673018, Kerala, India

²Inter-University Accelerator Centre, Aruna Asaf Ali Marg, New Delhi 110067, India

Energy of neutrons from Am-Be source was re-measured using g-tagged ToF method at very low detection threshold of 0.3 MeV [1]. $^{241}\text{Am}-^9\text{Be}$ source emits neutrons of energy up to 11 MeV through $\alpha+^9\text{Be} \rightarrow ^{13}\text{C} \rightarrow ^{12}\text{C}^*+n$ reaction induced by α -particles emitted by ^{241}Am . Energy of the emitted neutrons depends on the excited state of the ^{12}C formed with major contribution from the first excited state which has an energy of 4.44 MeV. Therefore, g-tagging provides an easy method to measure the energy of neutrons emitted from Am-Be source with good accuracy up to an energy of about 6.5 MeV. Neutrons emitted from the ground state of ^{12}C cannot be measured using this technique.

Neutrons were detected using a BC501A liquid scintillator detector and the associated g-rays were detected in a fast timing BaF_2 detector. The measurement was carried out in the NAND set up by keeping the source at the target position inside the spherical-shell scattering chamber. A g-detector was placed very close to the source at a distance of 3 cm and one of the BC 501A liquid scintillators in the horizontal plane of the NAND array was used to detect neutrons. The long flight path (175 cm) available in the NAND set up was an added advantage for measuring the neutron energy distribution with high resolution. The ToF distribution obtained between the g and neutron detector was used to produce the energy distribution of detected neutrons. Pulse shape discrimination based on zero-cross technique was employed to separate g events recorded by the liquid scintillator. In order to evaluate the effect of g-gating in the neutron energy measurement, total light output information from the liquid scintillator was also collected from the scintillator detector with and without g-tagging. The un-tagged light output has high energy neutron component as expected and can be clearly visualized in Figure 4.1.3. The experimental neutron energy spectrum was corrected for intrinsic detection efficiency of the detector, which was simulated using FLUKA [2]. The neutron energy distribution, thus obtained, was compared with that of the ISO 8529-2 standard neutron reference spectrum. Good agreement with measured data was observed in the overlapping energy range as shown in Figure 4.1.4. The present measurement extended lower energy range up to 0.3 MeV in comparison with the previous measurements using the same technique.

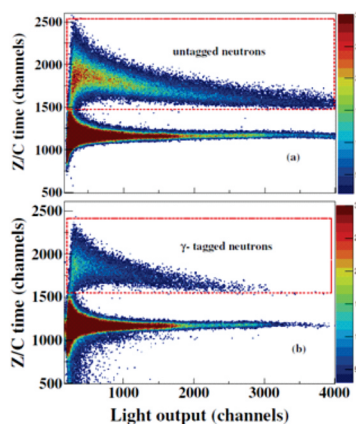


Fig. 4.1.3: Zero-cross vs. light output plots for g-untagged and g-tagged conditions. The figure is adapted from Ref. [1].

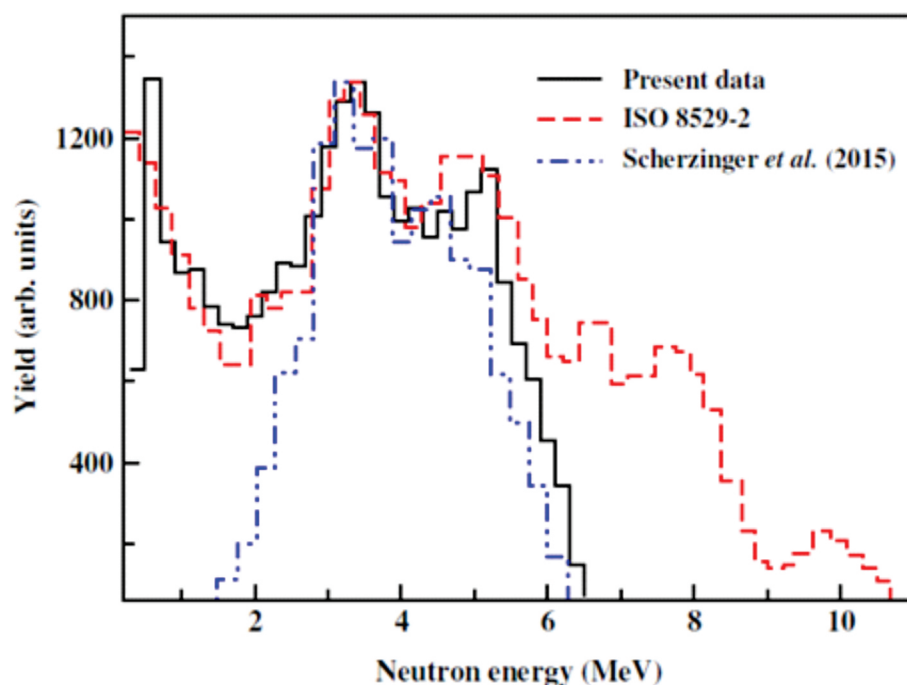


Fig. 4.1.4: Measured neutron energy distribution is compared with ISO standard [3] and earlier measurement by Scherzinger *et al.* [4]. The figure is adapted from Ref. [1].

REFERENCES:

- [1] F. S. Shana, K. S. Golda, N. Saneesh, D. Arora and P. Sugathan, *Applied Radiation and Isotopes* **193**, 110655 (2023).
- [2] Ferrari, A., Ranft, J., Sala, P.R., Fassò, A., 2005. FLUKA: A multi-particle transport code (Program version 2005). CERN-2005-10, CERN.
- [3] ISO-8529-2, 2000. International Organization for Standardization (2000) Reference neutron radiations, part 2: Calibration fundamentals of radiation protection devices related to the basic quantities characterizing the radiation field.
- [4] Scherzinger, J., Annand, J., Davatz, G., Fissum, K., Gendotti, U., Hall Wilton, R., Hakansson, E., Jebali, R.A., Kanaki, K., Lundin, M., Nilsson,

B., Rosborge, A., Svensson, H., *Applied Radiation and Isotopes* **98**, 74 (2015).

4.2 GAMMA DETECTOR ARRAYS: GDA and INGA

Yashraj, Indu Bala, R. Kumar, R. P. Singh and S. Muralithar

4.2.1 MADC testing

Yashraj, M. Jain, E. T. Subramaniam, R. P. Singh and S. Muralithar

Nine MADC-32 (4-INGA/GDA, 3-DSL and 2-HIRA/HYRA), procured from Mesytec, Germany were tested (Fig. 4.2.1) using a pulsar signal and HPGe Clover detector signal with ^{152}Eu source.

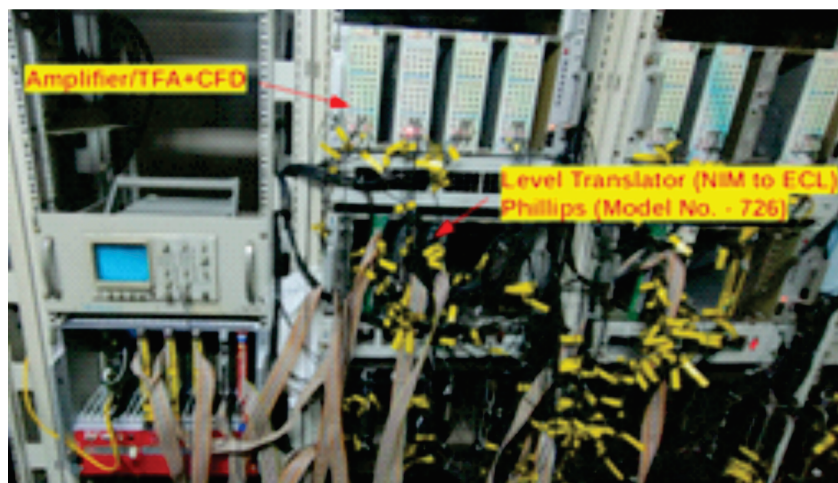


Fig. 4.2.1: Setup used for testing of MADCs

4.2.2 Biasing power supplies maintenance (5kV, 3kV and pre-amplifier)

S. K. Suman, Rajesh Kumar, Yashraj and Indu Bala

The Clover detector (5kV- 24 nos), ACS (3kV-18 nos) and pre-amplifier (8 nos) power supplies were removed from the two 19" racks placed in the INGA beamline. Then the racks as well as power supplies were cleaned using dry air. The faulty power supplies were serviced and after proper testing of all the supplies, NIM bins etc. the power supplies were placed back in the racks for smooth operation.

4.2.3 Annealing and evacuation

Yashraj, Indu Bala, R. Kumar, R. P. Singh and S. Muralithar

Eight Clover detectors were evacuated up to a pressure $\sim 10^{-7}$ mbar and annealed up to about 98 °C for improving their resolution.

4.2.4 Charged Particle Detector Array

A. Jhingan, M. Kumar, R. P. Singh, S. K. Saini, R. Ahuja, Yashraj, R. Kumar, Indu Bala and S. Muralithar

A newly-developed Charged Particle Detector Array (CPDA) consisting of 32 CsI detectors (16 backward + 16 forward) with home-made pre-amplifiers was integrated with the INGA array. After the successful beam-test, two user experiments were carried out. Clear identification of light charged particles like alpha and proton was achieved (Fig. 4.2.2), based on pulse shape discrimination.

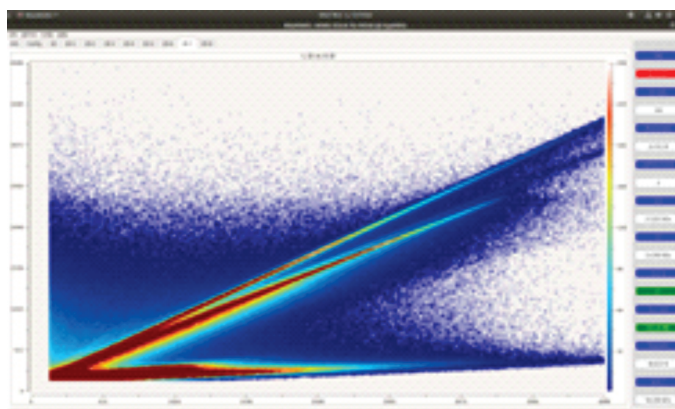


Fig. 4.2.2: Two-dimensional spectra obtained by plotting signals from CsI detector (long vs short shaping time).

4.2.5 Re-installation of Perturbed Angular Distribution facility in Phase-II

R. Kumar, U. S. Ghosh, G. K. Chaudhari, P. Barua, Chandra Pal, Indu Bala, Yashraj, T. Varughese, D. K. Prabhakar and D. K. Swami

The Perturbed Angular Distribution (PAD) facility was re-installed in the Phase-II atomic physics beamline to perform pending thesis experiments. The whole setup was uplifted from Beam Hall I with the help of the mechanical group and the beamline was redesigned to accomplish the set-up in Beam Hall II. The design consisted of an angular correlation table, a target chamber and a C-type electromagnet (to provide a maximum 1.8 T magnetic field between the 1" pole gap). Both types of detectors, scintillators and semiconductors, could be mounted in the plane perpendicular to the magnetic field. The setup is shown in Fig. 4.2.3. The aim was to systematically investigate the nuclear structure (configuration and the quadrupole deformation) and the decay mechanism of the K-isomers.

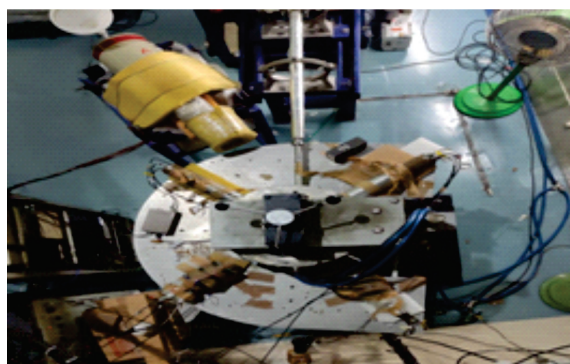


Fig. 4.2.3: PAD setup in Phase-II atomic physics beam line.

4.2.6 Enhancer module testing

A. Gupta, Yashraj, R. P. Singh, E. T. Subramaniam and S. Venkatramanan

One enhancer module was made and tested for long-term stability and time performance. This module enables collection of Compton-suppressed time signal from each crystal of the Clover detectors. Test results of peak-to-total and time performance were reported in the DAE Nuclear Physics Symposium.

4.2.7 Making glove box for servicing of HPGe Clover detectors

Yashraj, Indu Bala, Rakesh Kumar, S. K. Saini, R. P. Singh and S. Muralithar

A clean glove box (Fig. 4.2.4) with nitrogen environment for servicing HPGe Clover detectors was made. Detectors requiring FET or pre-amplifier replacement could be serviced in this box. The size of the glove box is $100 \times 98 \times 120 \text{ cm}^3$. Clover detectors can be put inside it through a door placed at one of the sides. Two gloves are put on one side from where the engineer will operate on the detector. An electrical connection is also provided inside the glove box to power lamps, soldering / de-soldering stations etc.



Fig. 4.2.4: Glove box for HPGe detector servicing.

4.2.8 Testing of amplifiers (MSCF-16) and ADC (MADC-32) received from Visva-Bharati

Indu Bala, R. P. Singh, S. Muralithar and Mamta Jain

Two amplifiers (MSCF-16), one ADC (MADC-32) and one TDC (MTDC-32) were received from Visva-Bharati, which would be used for INGA experiments at IUAC. We tested both the amplifiers and ADC with 416 pulse generator in the GDA beamline, with of 2 ms shaping time (maximum possible in these amplifiers). The resolution was about 0.06%, as expected. The ADC (MADC-32), integrated in the DAQ, was tested with ^{152}Eu and ^{60}Co sources in the INGA beam line. A resolution of $\sim 2.2 \text{ keV}$ was obtained for 1408 keV g-transition from ^{152}Eu .

4.2.9 BGO multiplicity filter for INGA

Indu Bala, S. K. Saini and S. Muralithar

BGO multiplicity filter assembly (Fig. 4.2.5), consisting of 14 bismuth germanate hexagonal crystals, was assembled for mounting in the INGA array in two groups (7 crystals in each), in 90° ring, at positions 11 and 15. These detectors were tested with g-source. The resolution was within 16% at 662 keV g-transition from ^{137}Cs .

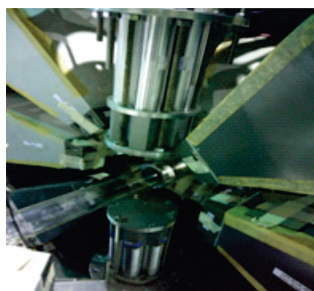


Fig. 4.2.5: BGO multiplicity filter in INGA.

The assembly was mounted in such a way that its distance from the glass tube could be adjusted as per the requirement and it could come close to the glass tube. The geometrical efficiencies were 8%, 24% and 62% at distances 14 cm, 8 cm and 5 cm, respectively. We kept a 2 mm thick SS plate in front of the crystals as a part of the assembly, to cut down the intensity of low energy X-rays (below 50 keV). Old electronics, to be used for this multiplicity filter, were tested with the pulser in the GDA beam line.

4.2.10 Re-routing of cables for LN₂ autofill system

R. N. Dutt, Yashraj, Indu Bala, R. Kumar and S. Muralithar

New sensors were mounted on the overflow valves and at the exit of Clover detectors. The new filling system was tested. Some more sensors are to be mounted to complete the task. Cabling for solenoid valves, sensors etc. were re-routed neatly through cable trays of the INGA beam line.

4.2.11 Setup for low activity civil-construction samples of IIT Roorkee

Yashraj and R. P. Singh

The low background studies for the samples (Phosphogypsum and flyash) from the Department of Civil Engineering, IIT Roorkee were performed using a Clover detector and processing electronics (Fig. 4.2.6). The data for 4 samples was collected for ~24 hours each. Analysis of data is under progress.



Fig. 4.2.6: Experimental setup used for data collection.

4.2.12 List of experiments performed in INGA/GDA facilities

S. No.	Title	PI	Duration	Institute	Facility
1.	CPDA facility test	Dr. R.P. Singh	27/05/2022 to 29/05/2022	IUAC, New Delhi	INGA
2.	PAD facility test	Dr. R. Kumar	02/06/2022 to 04/06/2022	IUAC, New Delhi	PAD/At. Phy
3.	Study of K-Isomers and high spin states in A = 180 mass region	Ms. Anupriya	17/06/2022 to 24/06/2022	Himachal Pradesh University, Shimla	INGA
4.	Nuclear structure studies of transitional nuclei in Mass A~85 region	Mr. Anuj	11/07/2022 to 16/07/2022	Delhi University	INGA
5.	Nuclear electromagnetic moment measurements in transitional nuclei near neutron shell closer N = 82	Ms. Anu Rathi	22/07/2022 to 28/07/2022	Panjab University	PAD/At. Phy
6.	Static electromagnetic moment measurements in neutron deficient iodine nuclei	Ms. Ritu Rani (2 runs)	12/08/2022 to 27/08/2022	Panjab University	PAD/At. Phy
7.	Nuclear electromagnetic moment measurements in transitional nuclei near neutron shell closer N=82	Ms. Anu Rathi (2 nd run)	28/08/2022 to 03/09/2022	Panjab University	PAD/At. Phy
8.	Study of transitional nuclei in A~100 region	Mr. Kaushik Katre	08/09/2022 to 14/09/2022	IUAC, New Delhi	INGA

S. No.	Title	PI	Duration	Institute	Facility
9.	CPDA facility in-beam test	Dr. R.P. Singh	18/10/2022 to 20/10/2022	IUAC, New Delhi	INGA+ CPDA
10.	Gamma ray spectroscopy of some astrophysically important nuclei towards endpoint of nova nucleosynthesis	Mr. Subodh	21/10/2022 to 29/10/2022	Panjab University	INGA+ CPDA
11.	Study of heavy-ion induced incomplete fusion reactions dynamics at energy below 10 MeV/nucleon	Mr. Sushil Kumar	31/10/2022 to 07/10/2022	IUAC, New Delhi	INGA+ CPDA
12.	High spin structure and lifetime measurements using Recoil Distance Doppler Shift method in mass region A~120 nuclei	Ms. Bharti Rohilla (2 runs)	14/11/2022 to 23/11/2022	Panjab University	INGA
13.	High spin states and life-time measurements in mass region A~ 100 nuclei using Recoil Distance Doppler Shift Method	Ms. Diwanshu Sharma (2 runs)	21/12/2022 to 30/12/2022	Panjab University	INGA
14.	Lifetime measurement study of octupole deformation in neutron deficient nuclei of mass A~120	Mr. Anand Pandey	01/01/2023 to 06/01/2023	Delhi University	INGA+ Plunger

4.3 Recoil Mass Spectrometers

4.3.1 Heavy Ion Reaction Analyzer (HIRA)

S. Nath, J. Gehlot, Gonika, T. Varughese and N. Madhavan

HIRA facility was used in a student thesis experiment (Ms. Anjali Rani, University of Delhi) which involved transfer cross section measurements in the systems $^{28}\text{Si}+^{116,120,124}\text{Sn}$ around the Coulomb barrier. These measurements supplemented those of fusion evaporation residue (ER) and quasi-elastic back-scattering cross sections carried out last year in the HIRA. The recently commissioned VME-based data acquisition system was used in this experiment. As several experiments were taken up in the HIRA in the previous year, the pending thesis experiments in HYRA were given priority this year as per the waiting list in the AUC-sanctioned experiments.

Seven papers were published in the period April 2022 to March 2023 (five in Physical Review C and two in The European Physical Journal A) based on thesis experiments carried out in the past couple of years using the HIRA.

4.3.2 HYbrid Recoil mass Analyzer (HYRA)

N. Madhavan, S. Nath, J. Gehlot, Gonika and T. Varughese

HYRA facility was used in the gas-filled mode in the following facility test and student thesis experiments during this year. Beams from Pelletron accelerator were used in all the experiments as there was no SC-LINAC operational cycle in the past year.

(1) Facility test of the newly commissioned VME-based data acquisition system in the HYRA facility was carried out with beam, with close coordination of the Data Acquisition System group who had indigenously developed the software and some of the hardware.

(2) ER cross-section measurements for the systems $^{30}\text{Si}+^{140}\text{Ce}$ (energies above as well as below the Coulomb barrier) and $^{32}\text{S}+^{138}\text{Ba}$ (energies below the Coulomb barrier), both forming the same compound nucleus, $^{170}\text{Hf}^*$, were successfully carried out. These measurements were based on the thesis proposal by Ms. Malvika of IIT Roorkee, to study possible entrance channel effects. The above barrier energy measurements in the latter system are planned in the next SC-LINAC operational cycle.

(3) ER cross section measurements for the system $^{30}\text{Si}+^{142}\text{Ce}$ (above as well as below the Coulomb barrier) were carried out as part of the thesis proposal by Ms. Amninderjeet Kaur of Panjab University, Chandigarh.

Another system $^{48}\text{Ti}+^{124}\text{Sn}$, forming the same compound nucleus ($^{172}\text{Hf}^*$) but which requires higher beam energies for populating with similar excitation energies, is planned to be taken up in the forthcoming SC-LINAC operational cycle. In order to experimentally extract the ER transmission efficiency, $^{28}\text{Si}+^{142}\text{Ce}$ was used as the calibration system at a few energies for which the ER cross sections were already available.

A paper was published in Physical Review C and another was communicated based on thesis experiments carried out using the HYRA in the past couple of years. A few experimental proposals were submitted and successfully defended by research scholars from various universities in the two AUC meetings at IUAC in 2022, with the help of HIRA/HYRA group.

Mr. Chandra Kumar (Research Scholar) won one of the best poster presentation awards in the DAE Symposium on Nuclear Physics SNP-2022 held at Cotton university, Guwahati, Assam in December 2022 as well as the first prize for presenting a poster in Nuclear Reaction and Structure up to Intermediate Energy Collision NRSIC-23 held at VECC, Kolkata in January 2023.

4.4 MATERIALS SCIENCE FACILITIES

A. Tripathi, D. Kabiraj, F. Singh, V. V. Sivakumar, S. A. Khan, I. Sulania, S. K. Kedia, R. C. Meena and A. Mishra

The Materials Science facilities are supporting research programmes of a large number of users from different Universities and research Institutions. There were nearly 57 beam time experiments carried out for Materials Science Users. Out of these, 50 experiments were carried out in BH-1, 07 experiments were carried out in BH-2. In total, 125 shifts have been utilized by the users for their beam time irradiation experiments.

4.4.1 Irradiation Chamber in Beam Hall I

Many maintenance activities were undertaken this year and a few of them are described.

4.4.1.1 Rotary Stage Leak

I. Sulania, SA Khan, P Barua and A. Tripathi

The rotary stage (MDC RMTG-600) above the irradiation chamber to rotate the sample ladder

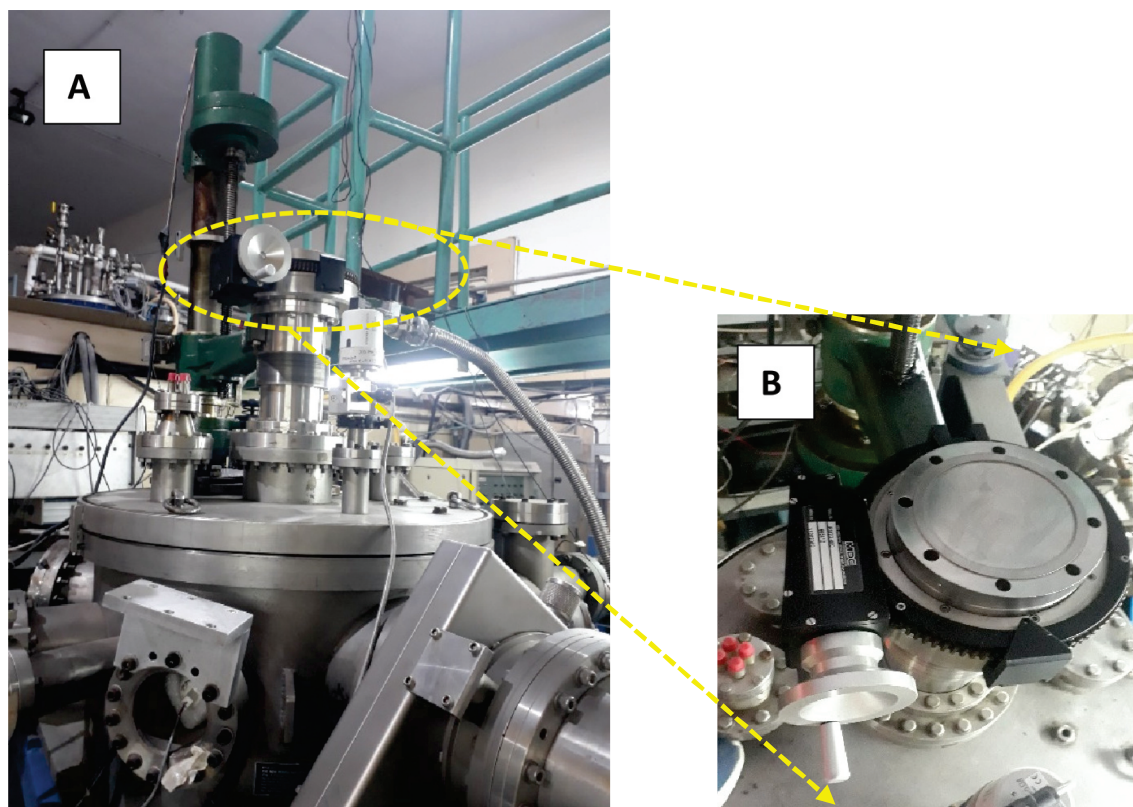


Figure 1: (A) Rotary stage (RMTG-600, MDC make) connected to the chamber (B) Top view

(without breaking the chamber vacuum) developed a minor leak which became evident due to deterioration in the chamber vacuum at the time of ladder rotation in Sept. 2022. Chamber vacuum was tested with the blank off to ensure that the leak is not related to chamber. As a temporary emergency measure, a separate differential pumping arrangement was made by Vacuum Lab to facilitate the completion of beam time experiments (Figure 2). Many experiments have since taken place without any vacuum deterioration in the experimental chamber during experiments.

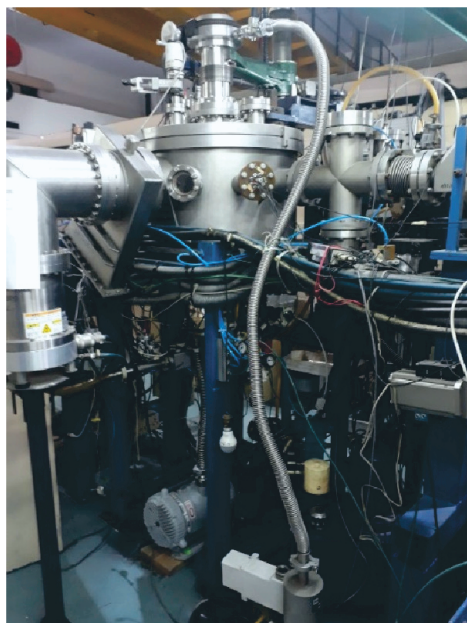


Figure 2: Separate differential pumping arrangement for the rotary stage.

The rotary stage will be replaced with a new one with similar dimensions, for smooth functioning during the beam time experiments.

4.4.1.2 As a follow up of the Safety committee feedbacks, a check list is put up in the beam line in BH-1 for the users to ensure that all the steps are followed properly during the beam time experiments.

4.4.1.3 A test run was conducted by Health Physics Group for radiation monitoring in the Mat Sci. beam line area with Au ion beam in Dec. 2022.

4.4.2 Centre for Materials Characterization and Measurement (CMCM)

S. A. Khan, S. K. Kedia, R. C. Meena, A. Tripathi

A new Centre for Materials Characterization and Measurement (CMCM) is being established at IUAC which will house all the offline facilities for materials characterization and measurement at one place. The area for CMCM in LEIBF building of IUAC was renovated and the identified instruments were moved to the respective assigned places this year.



Figure 1. A photograph of the main hall in CMCM area with solar simulator, FTIR, UV-Vis-NIR spectrophotometer, UV-Vis spectrophotometer, contact angle measurement setup, optical microscope, and photoluminescence setup (left to right).

Some of the instruments associated with this centre are shown in the main hall of the CCM facility on the first floor (Figure 1). The other characterization instruments installed in other rooms of the CCM facility are Atomic Force Microscope, Transmission Electron Microscope, Scanning Electron Microscope, Hall Effect setup, setup for Transport Measurements (IV, CV, Dielectric, conductivity), and Semiconductor Analyzer. Also, there are instruments for sample preparation viz, Sputtering system, Thermal Evaporation, Sputter Coater, Furnaces, Rapid Thermal Annealing, and ECR deposition. The facilities proposed for the future include x-ray diffractometer, VSM, AFM/Raman, MOKE, P-E loop, and gas sensing setup.

As suggested by the governing body, IUAC is planning for the accreditation of CCM as per the ISO norms. This will attract and help R&D labs, industrial R&D entities, MSMEs, Incubators, Startups etc. apart from catering to the needs of IUAC accelerator users. Therefore, the centre also plans to provide technical help and scientific knowledge to the end users interested in utilizing these sophisticated scientific instruments. In this direction, a workshop will be organized in the last week of October 2023 on characterization techniques.

4.4.3 Materials Synthesis and Microscopy laboratory

I. Sulania, S.A. Khan, V V Sivakumar and A. Tripathi

The renovation and reorganization works was carried out in the laboratory over the year. The different systems which were present in the laboratory were shifted out and re-assembled after epoxy flooring work was done. An e-beam evaporation system was shifted into the laboratory area. The laboratory has many synthesis facilities for the growth of thin films and nano-powders as well as characterization facilities such as Scanning Electron Microscope, Scanning Probe Microscope, Optical Microscope, UV-Vis Spectrophotometer, and Contact Angle measurement set-up. The facilities are in proper working condition. The Microscopy facilities have been extensively utilized by the IUAC user community belonging to different universities/institutes.

4.4.3.1 Scanning Electron Microscopy

S. A. Khan, I. Sulania and A. Tripathi

The electron emitter of TESCAN's MIRA II LMH Field Emission Scanning Electron Microscope (FE-SEM) reached its end of life in February 2022. A new electron emitter was procured and installed through TESCAN's authorized Indian Agent in March 2023. The system along with the attached Energy Dispersive X-ray Spectroscopy attachment from Oxford Instruments is now working satisfactorily.

4.4.3.2 Scanning Probe Microscope

I. Sulania and A. Tripathi

Most of the Scanning Probe Microscope modes such as AFM, MFM, C-AFM, STM, STS and F-d mode, etc. are available at IUAC and used in user experiments. The facility is working satisfactorily. There was a problem with top plate of J Scanner head (Figure 1).



Figure 1: Photograph of J Scanner with top plate.

The scanner's top plate came out with sample puck and the same is to be fixed carefully as there is a small O-ring that insulates it from the main body. To continue with the user support, the E scanner is presently being used for the measurements and the same was calibrated with a standard sample. The E-scanner scans up to $\sim 13 \times 13$ micrometer (Figure 2). The facility is being used rigorously for User Support. In total, there were ~ 275 samples characterized for 58 users in AFM/MFM mode out of which 256 were in Tapping mode AFM and 19 in MFM mode.

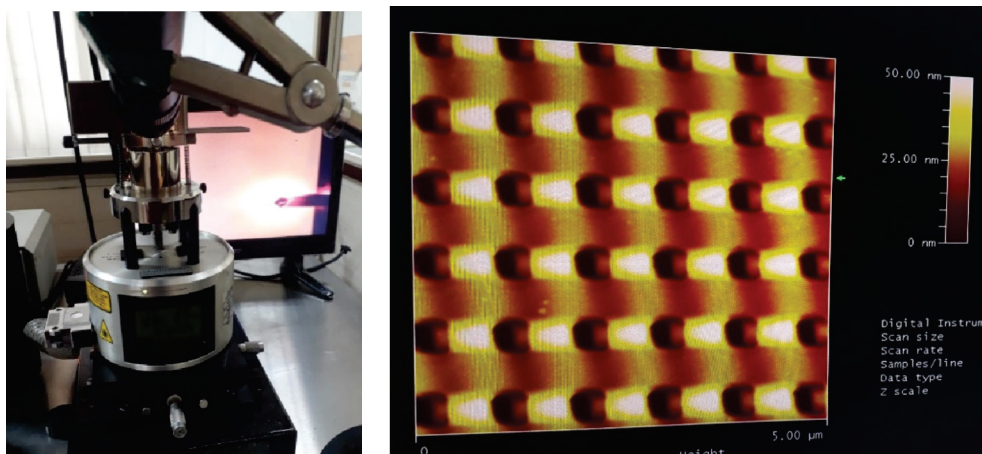


Figure 2: AFM with E scanner and image of the standard sample.

4.4.3.3 Optical Microscope

I. Sulania and A. Tripathi

The laboratory has a high-end 100X Optical Microscope from Zeiss, which is mostly used as a tool to predetermine the sample's area before performing the SPM measurements. It is especially useful for preliminary studies in samples showing distinct colour contrasts such as in single or multilayer graphene flakes etc. The Optical Microscope system was utilized for characterizing 5 samples of 2 users.

4.4.3.4 The UV-Vis Spectrophotometer

I. Sulania and A. Tripathi

UV-Vis Spectrophotometer, which was procured from Hitachi, is capable of doing measurements in Absorbance/Transmission mode. The UV-Vis spectrophotometer was used to characterize 120 samples of 15 users

4.4.3.5 Contact angle measurement facility

I. Sulania

Drop Shape Analyzer, DSA100, from Kruss GmbH, Germany is a high-quality system for knowing the wetting and adhesion properties of solid surfaces as the contact angle (wetting angle) is a measure of the wettability of a solid by liquid. This year, it was utilized by 8 users scanning nearly 80 samples. The set-up is working satisfactorily and no major maintenance was required.

4.4.4 Transport Lab

R. C. Meena and A. Tripathi

The transport lab facilities are extensively used to characterize the type of conduction nature, charge carriers and their concentration, charge storage ability and the thermoelectric ability of a material, etc. The characterizations are performed on both bulk materials as well as on thin films. To check the temperature-dependent measurement, a liquid nitrogen-based dip-stick bath (temperature range 80-450 K) and close-cycle refrigerator (CCR) (temperature range 20-300 K) are used and the temperature is varied using the commercial temperature controller. The temperature-dependent measurements are performed in the vacuum of the order of 10^{-3} mbar. The type of conduction nature is checked by measuring the temperature dependence resistivity using the source meter or electrometer. Both Two-probe and four-probe measurements are performed on these samples as necessary. The type of charge carriers and their concentration are determined using the Hall effect measurement system. The charge storage ability and its frequency dependence (20 Hz-2 MHz) are determined using the LCR meter. The semiconductor devices are studied using the current-voltage (I-V), Capacitance-voltage (C-V) type of measurements using the Semiconductor Device Analyzer. The

thermoelectric efficiency of the samples is studied using the in-house developed thermoelectric setup and the measurement is performed on both bulk as well as on thin film using differential method. All these characterizations are performed using user-friendly LabVIEW-based computer programmes. The facilities are calibrated regularly using various standard samples. More than 57 users from various universities/institutes utilized these facilities.

The in-situ transport measurement facility is also available in the BH-1. The various type of semiconductor devices like diodes, BJT, and MOSFET are characterized with varying fluence and energy of the incident ion-beam. The in-situ measurement is also available at liquid nitrogen temperature as well as higher temperatures. This year two in-situ experiments were performed in BH-I.

4.4.5 High-Resolution Transmission Electron Microscopy (HRTEM)

A. Mishra, Abhilash S.R. and D. Kabiraj

IUAC TEM and TEM sample preparation facilities are being utilized by various users of different universities.

4.4.5.1 TEM Specimen Preparation Facility

The TEM specimen preparation facility is equipped with an Ultrasonic bath, Hot Plate, Traditional Lapping/Grinding Tools, Dimple Grinder, Diamond Wire Saw, and Precision Ion Polishing System (PIPS). All these instruments are regularly used for TEM sample preparation. Planar TEM, Cross-sectional TEM (XTEM), and Powder samples on TEM Grids are prepared for TEM characterization. The TEM specimen preparation facility has been utilized to prepare more than 107 TEM samples including 11 XTEM and 26 planar samples by various users during this academic year 2022-2023.

4.4.5.2 High-Resolution Transmission Electron Microscope (HRTEM) Facility

Maintenance of TEM is very important for smooth operation and is done as and when required. Some of the regular TEM maintenance activities undertaken are the Bake-out process followed by HT conditioning, ACD heating, Camera warmup, etc. TEM Bake-out cycle has been performed in the month of June, September, December 2022, and February 2023. More than 110 samples of various users have been characterized for TEM, HRTEM, SAED, STEM-EDS, and STEM-EELS.

4.4.5.3 Some of the research works published during 2022-2023 in peer-reviewed journals using the IUAC TEM facility are listed below:

4.4.5.3.1 Morphological, and structural characterization of amorphization/ crystallization at the interfaces of thin films and within the semiconductor systems

Anusmita Chakravorty et. al studied ionization-stimulated damage recovery in GaAs system [1]. In this study, controlled damage has been introduced using 300 KeV Ar ion irradiation, followed by successive irradiation using 100 MeV Ag ions at ~ 80 K by varying the fluence (ions cm^{-2}). The 3D version of the thermal spike model (TSM) has been used to simulate the temperature profiles after an impact of SHI irradiation on an amorphous nano-zone embedded in a crystalline GaAs matrix. 3D-TSM simulations have predicted that the thermal spike in this zone was confined, indicating melt-flow at the crystalline-amorphous interface that could promote recovery. This lattice recovery has been supported by XTEM results (as shown in Fig. 1).

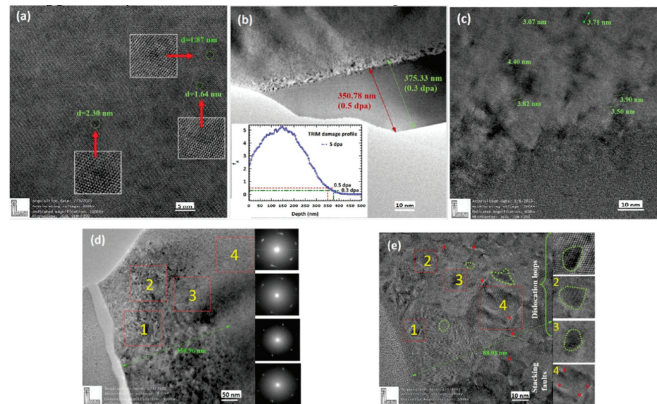


Fig. 1: Cross-sectional TEM images of the GaAs crystal irradiated with (a) 6.9×10^{13} (0.3 dpa) and (b) 1×10^{15} ion cm^{-2} (5 dpa). (c) TEM image of (b) at a higher magnification, recorded at a depth of around 350 nm, displaying details of the small dark areas up to the atomic level. (d) TEM image of GaAs crystal irradiated with 1.2×10^{14} ion cm^{-2} (0.5 dpa), followed by sequential irradiation with 100 MeV Ag at ~ 80 K with 3×10^{13} Ag cm^{-2} . Insets present the fast Fourier transforms (FFTs) of some selected regions. (e) Higher magnification image of (d). Insets in (a) and (e) present the zoom-in view of the selected regions "[1].

G. Maity et. al presented a novel technique to develop poly-crystalline Si thin films at room temperature using 500 keV Xe⁺ ion irradiation [2]. The Al-induced crystallization process has been employed to reduce the crystallization temperature. For that, c-Al (50 nm)/a-Si (150 nm) bilayer thin films have been used for irradiation experiments. Structural studies have shown that crystallization of Si was started at a threshold fluence of 3×10^{15} ions cm⁻², and crystallinity was found to increase with increasing ion fluence. XTEM study has been shown in Fig. 2. A similar kind of detailed review study of metal-induced crystallization of a-Si and a-Ge thin films has also been published by G. Maity et. al [3].

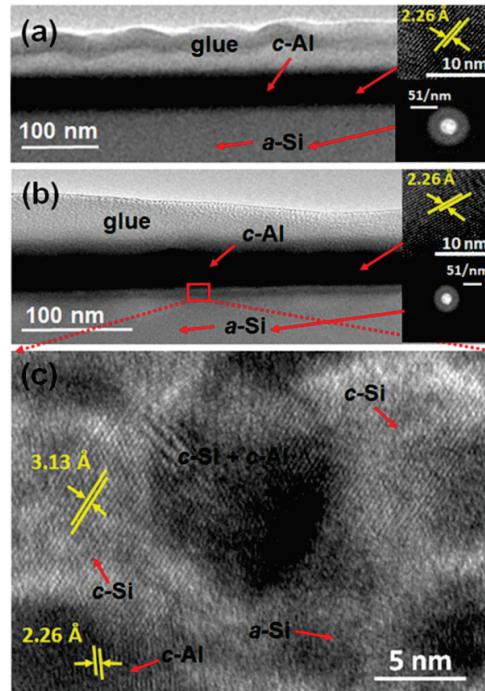


Fig. 2: XTEM micrograph of the (a) pristine sample and (b) the sample irradiated at a fluence of 1×10^{16} ions cm⁻². (c) High-resolution TEM (HRTEM) image of a selected area of the interface [2].

4.4.5.3.2 Study of morphological and structural properties of 2D materials

Rohit Sharma et. al has demonstrated a simple drop cast method for the fabrication of MoS₂ and WS₂ channel-based FET on commercially available pre-patterned OFET devices [4]. The synthesis of few-layers thick MoS₂ and WS₂ nanosheets (NSs) has been done by solvent-assisted exfoliation method. A large number of thin flakes of MoS₂ and WS₂ have been shown in the TEM images shown in Fig. 3 (a) and (b), respectively. The regular lattice fringes of MoS₂ with an interplanar distance of ~ 0.251 , ~ 0.206 and ~ 0.204 nm correspond to the planes (012), (006) and (014), respectively have been shown in the HRTEM image in inset of Fig. 3 (a). Similarly, the regular lattice fringes of WS₂ with an interplanar distance of ~ 0.263 and ~ 0.296 nm corresponding to the planes (011) and (004) respectively have been shown in the HRTEM image in inset of Fig. 3 (b). The SAED image, inset of Fig. 4 (a), and the FFT image, inset of Fig. 3 (b), confirm the polycrystalline nature of MoS₂ and WS₂ nanosheets, respectively.

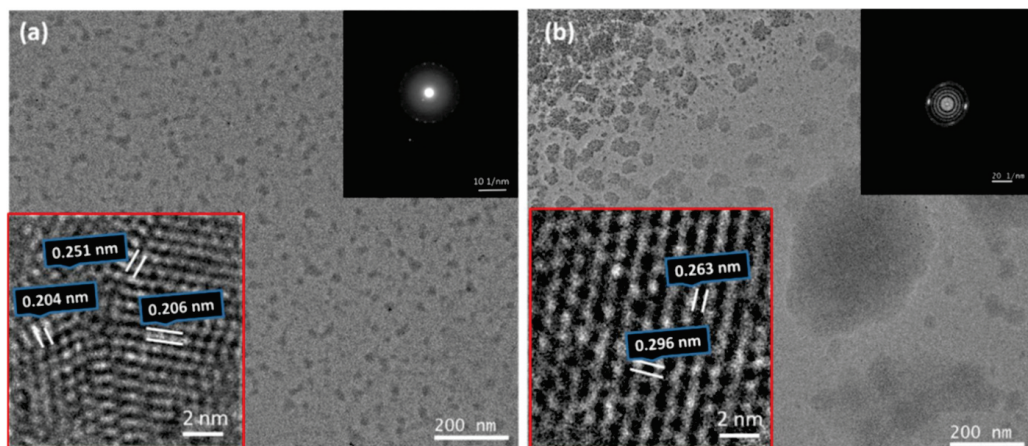


Fig. 3: TEM images of (a) MoS₂ NSs, and (b) WS₂ NSs. The inset images of Fig. 4(a) show the HRTEM and SAED images.

On the other hand, the inset images of Fig. 4(b) show the HRTEM and FFT images – [4].

4.4.5.3.3 Morphological and structural characterization of thin films, powder samples, and embedded systems

Hemant Jatav et. al has synthesized the nanocomposites (NCs) of Ag NPs inside the silica matrix using the atom beam co-sputtering technique. The post-deposition growth of the embedded Ag NPs has been systematically investigated at a wide range of annealing temperatures (ATs)[5]. HRTEM images of the NC samples annealed at different temperatures have been shown in Fig. 4. The images show the size, shape, and distribution of NPs inside the silica matrix. From these images, it has been found that the majority of Ag NPs are spherical in shape and their size distribution changes with AT. The mean size of stable spherical NPs in the as deposited sample has been estimated to be $\sim 5.0 \pm 1.6$ nm as shown in Fig. 4(a). For annealed samples, the average size of the spherical NPs has been found to be $\sim 4.8 \pm 1.3$ and $\sim 4.9 \pm 0.9$ nm for 400 and 600 °C annealed samples presented in Fig. 4(b) and Fig. 4(c), respectively.

The calculated d-spacing has been found to be in the agreement with the literature, and it corresponds to the (111) crystal plane of Ag NPs. On the other hand, the mapping of the constituent elements have been conducted through STEM-EDX as shown in Fig. 5, which confirms the existence of Ag NPs inside the silica matrix[5].

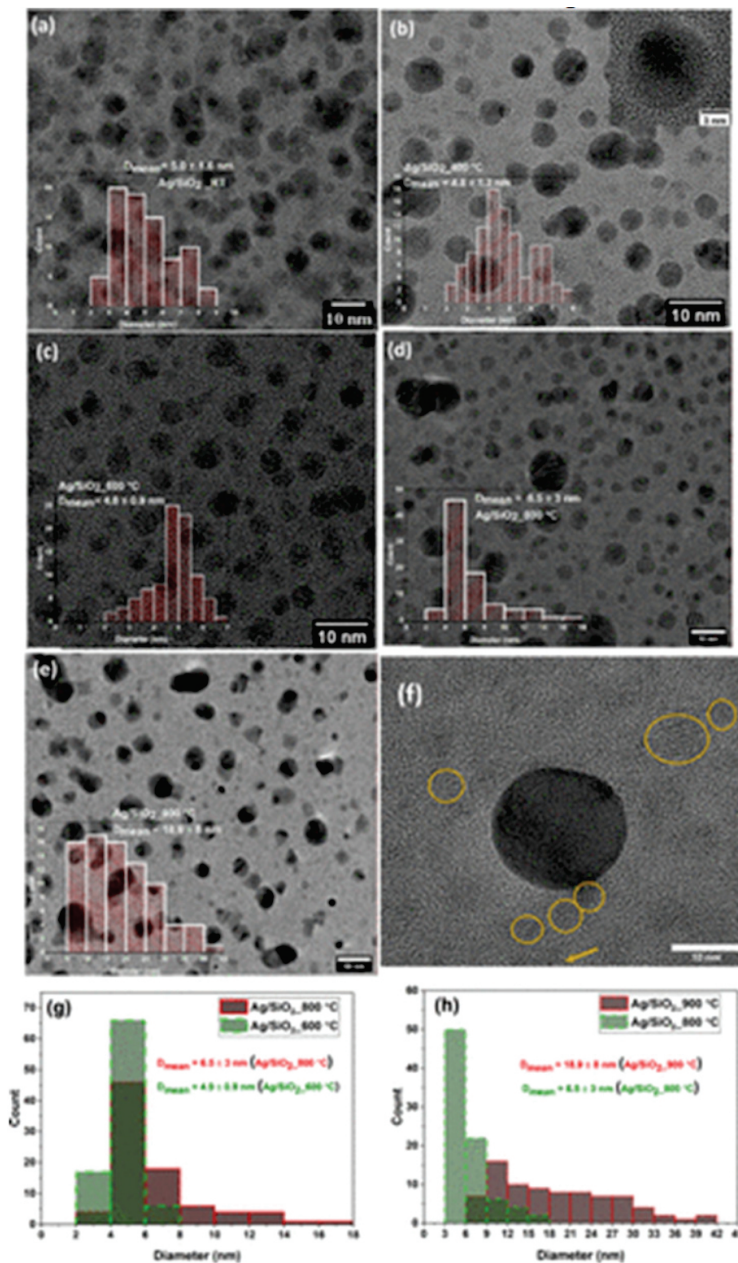


Fig. 4: HRTEM images of Ag nanoparticles (NPs) inside silica matrix at (a) 25 (as deposited) (b) 400, (c) 600, (d) 800, and (e) 900 °C. (f) HRTEM image of the 900 °C annealed sample (yellow circle indicates the presence of small nanoclusters) and the histograms in the inset show the mean size and distribution of NP size with different annealing temperatures. (g, h) Comparison of histograms at different annealing temperatures [5].

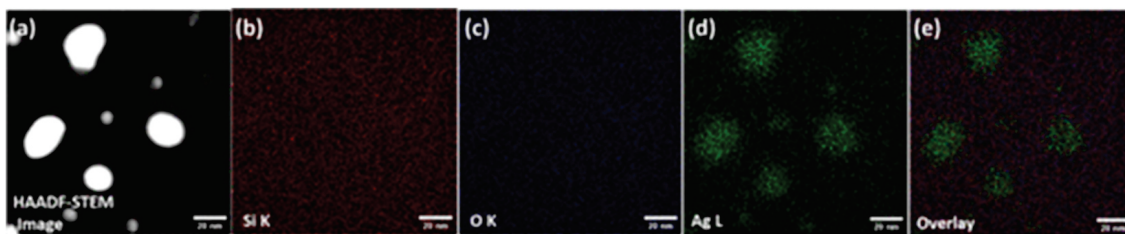


Fig. 5: (a) HAADF-STEM images of Ag nanoparticles (NPs) inside the silica matrix at 800 °C. Scanning TEM energy-dispersive X-ray spectroscopy elemental mapping of (b) silicon-K, (c) oxygen-K, and (d) silver-L edge. (e) Overlay of images (b–d). It indicates that silicon and oxygen are distributed uniformly throughout the nanocomposite thin film, whereas silver is present in the form of nanoparticles, which are mostly spherical in shape [5].

Jitender Kumar et. al has synthesized Cu-doped $\text{Mg}_2\text{B}_2\text{O}_5$ nanophosphors using a combustion method, and investigated their structural, morphological, optical band gap, electronic structure, and photo/thermo-luminescence properties using XRD, SAED, HRTEM, DRS, XANES, PL, and TL glow curves [6]. TEM images showed the formation of elongated, non-uniform, asymmetric, and agglomerated nanocrystals with a size range between 55 nm and 126 nm and average particle size as 80 nm, as shown in Fig. 6. The HRTEM images have been analysed using Image-J software, and the calculated d spacing has been found to be corresponding to the lattice plane (110) of triclinic $\text{Mg}_2\text{B}_2\text{O}_5$ nanophosphors. SAED has also been carried out, and the calculated d-spacing has been found to be corresponding to (120) of triclinic $\text{Mg}_2\text{B}_2\text{O}_5$ [6].

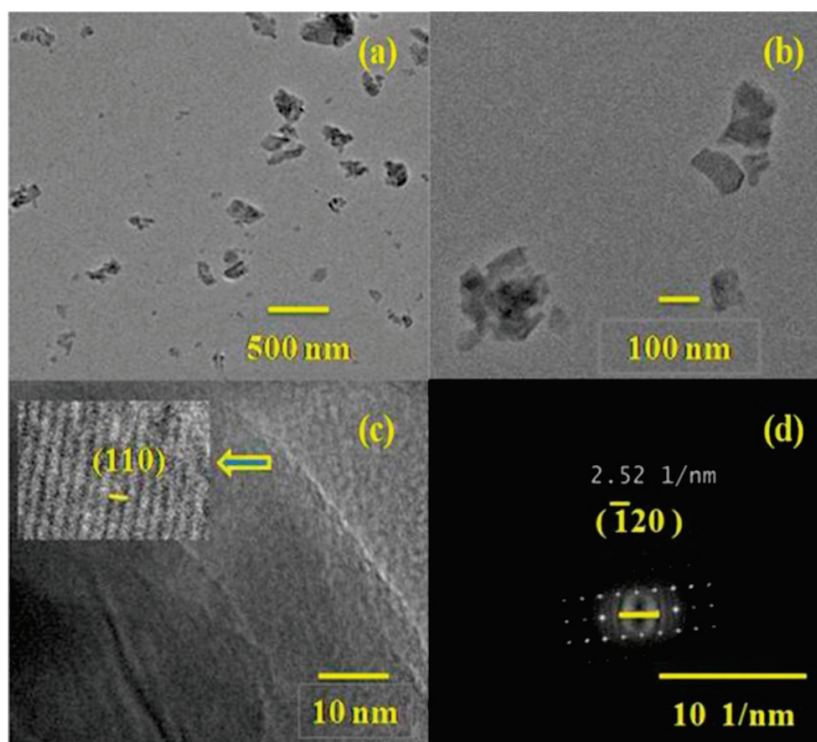


Fig. 6: (a) TEM image, (b) magnified TEM image, (c) HR-TEM image, and (d) SAED pattern of Cu (0.3%) doped $\text{Mg}_2\text{B}_2\text{O}_5$ nanophosphors [6].

Sapna Yadav et. al has synthesized the NiO/ Cr_2O_3 nanocomposite by a simple chemical reduction method to study its photo-catalytic activity under sunlight irradiation [7]. The TEM images have revealed that the synthesized NiO/ Cr_2O_3 nanocomposite was stable after five cycles of photocatalytic reaction [7].

Shraddha Shukla et. al has synthesized the ZnO nanoparticles by the precipitation method and characterized further by UV–Vis, FTIR, XRD, FE-SEM, and TEM. This research has disclosed degradation of three most commonly used antibiotics, i.e., amoxicillin (AMX), azithromycin (AZT), ofloxacin (OFX), and their consortium, using ZnO nanoparticles as a photocatalyst and UV light as a source to activate photocatalyst [8]. In Fig. 7(A) and (B), the TEM images of ZnO nanoparticles have been shown at different scales 500 and 100 nm, respectively. The grain size of the nanoparticle has been measured to be ~20 nm as shown through histogram in Fig. 7(B).

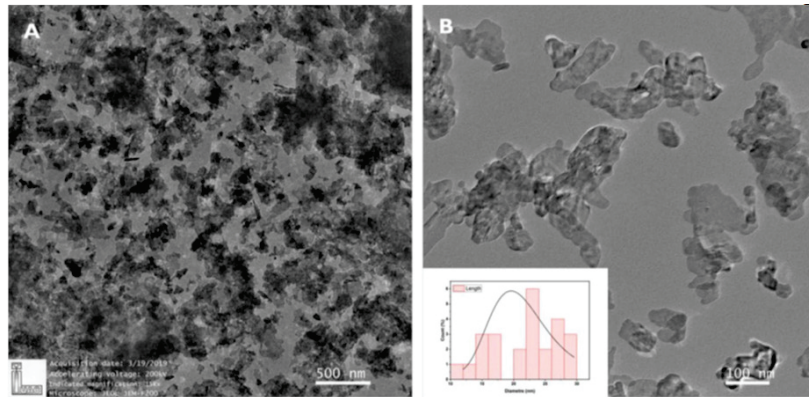


Fig. 7: TEM images of ZnO nanoparticles at different scales: (A) 500 nm, (B) 100 nm – [8]

From the HRTEM images in Fig. 8(A) and (B), the lattice spacings have been found to be 0.192 nm, 0.278 nm, and 0.163 nm corresponding to the hkl planes (102), (002), and (110), respectively [8].

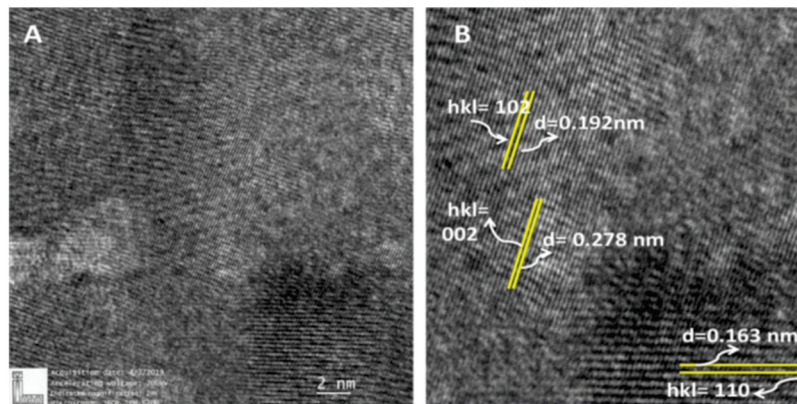


Fig. 8: HRTEM images of ZnO nanoparticles at (A) 2 nm (B) d-spacing and hkl planes – [8]

Prashansa Singh et. al has investigated in detail the laser-mediated upconversion emission and temperature-sensing capability of $(\text{Ca}_{0.99-a}\text{Yb}_{0.01}\text{Er}_a)\text{TiO}_3$. Samples have been prepared at different concentrations to observe the effect of erbium on upconversion while increasing its concentration and keeping all the other parameters constant [9]. The TEM micrograph in Fig. 9(a) has confirmed the spherical morphology of the particles and shown that the crystallites are agglomerated due to annealing performed at high temperature (900 °C) [9]. The SAED pattern of the Er^{3+} - Yb^{3+} codoped CaTiO_3 nanocomposite has confirmed the polycrystalline nature with the lattice planes (130), (221), and (111) as shown in Fig. 9(b).

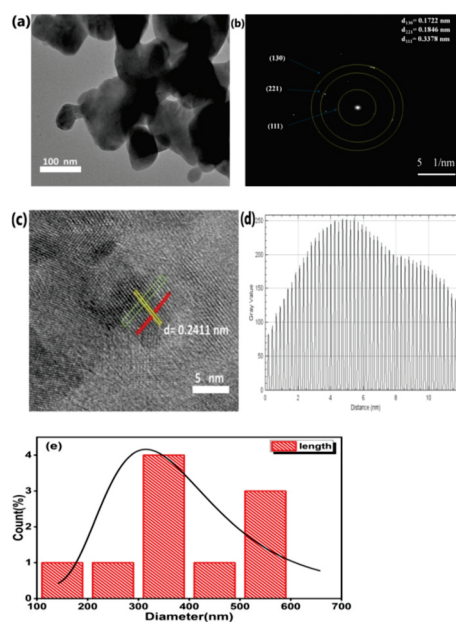


Fig. 9: (a) Transmission electron microscopy image of $\text{CaTiO}_3: 1 \text{ at}\% \text{Er}^{3+}, 1 \text{ at}\% \text{Yb}^{3+}$, (b) corresponding SAED pattern, (c) corresponding HRTEM image, (d) fringes of lattice spacing and (e) size distribution histogram plot [9].

References

- (1) A. Chakravorty, C. Dufour, A. Mishra, D. Kanjilal, D. Kabiraj, *J. Phys. D: Appl. Phys.* 55 (2022).
- (2) G. Maity, R. Singhal, S. Ojha, A. Mishra, U.B. Singh, T. Som, S. Dhar, D. Kanjilal, S.P. Patel, *J. Appl. Phys.* 132 (2022).
- (3) G. Maity, S. Dubey, T. Meher, S. Dhar, D. Kanjilal, T. Som, S.P. Patel, *RSC Adv.* 12 (2022) 3389933921.
- (4) R. Sharma, A. Kumar, A. Dawar, S. Ojha, A. Mishra, A. Goyal, R. Laishram, V.G. Sathe, R. Srivastava, O.P. Sinha, *Trans. Electr. Electron. Mater.* 24 (2023) 140148.
- (5) H. Jatav, M. Shabaninezhad, M. Mićetić, A. Chakravorty, A. Mishra, M. Schwartzkopf, A. Chumakov, S. V. Roth, D. Kabiraj, *Langmuir* 38 (2022) 1198311993.
- (6) J. Kumar, A. Sharma, S.O. Won, K.H. Chae, C. Shekhar, S. Kumar, A. Vij, *J. Electron. Mater.* 51 (2022) 19221932.
- (7) S. Yadav, N. Rani, K. Saini, *Environ. Sci. Pollut. Res.* (2022).
- (8) S. Shukla, H. Pandey, P. Singh, A.K. Tiwari, V. Baranwal, J. Singh, A.C. Pandey, *Brazilian J. Phys.* 52 (2022) 19.
- (9) P. Singh, N. Jain, S. Shukla, A.K. Tiwari, K. Kumar, J. Singh, A.C. Pandey, *RSC Adv.* 13 (2023) 29392948.

4.4.6 Structure and Spectroscopy Lab

S. K. Kedia, and F. Singh

The laboratory is having several research facilities for the development and characterizations of materials namely RF sputtering, e-beam evaporator, tubular furnace, high temperature furnace, in-situ micro-Raman spectrometer, in-situ X-ray diffractometer, UV-Vis-NIR spectrometer, FTIR, photo-luminance spectrometer, solar simulator, etc. These research facilities have been extensively used by the many researchers. However, many of them are having aging issues. Therefore, the regular operation and upkeep is becoming challenging issue. The micro-Raman facility has been down for quite some time and some tests have been carried out with the support of service engineer on the old XP based system only and it will be available for the users shortly. The PL system installation is also being planned.

4.4.6.1 X-Ray Diffraction System

S. K. Kedia, F. Singh and A. Tripathi

The XRD system is operational for approximately 17 years in Beam Hall-2. And its service and maintenance is being handled indigenously. Several alarms, faults, glitches are being addressed in-house on a regular basis. A series of MoS₂ thin films were characterized in the presence of controlled gas environment. XRD patterns have been recorded using in-situ XRD facility equipped with Cu^{K_α} source with wavelength 1.54 Å (40 kV and 40 mA power), Gobel mirror and scintillator detector. This facility allows us to record diffraction pattern in the controlled gas atmosphere. MoS₂ films were exposed to different concentrations of H₂ gas (3% and 100%) mixed with noble gas Argon (Ar) one by one after different intervals of pressure ranging from 50 mbar to 900 mbar. Data was recorded in locked coupled mode in the scan range of 2θ from 10° to 60° with step size of 0.02° at a scan speed of 0.25°/min. Similarly, the low-temperature XRD setup has also been assembled and tested, the detailed analysis of the same is under process by user.

4.4.6.2 Shifting, re-installation and utilization of UV-Vis-NIR and FTIR facilities

J. Yadav, S.K. Saini, G.K. Chaudhury, S. K. Suman, R. C. Meena, Sanjay K. Kedia, S.A. Khan, and F. Singh

The UV-Vis-NIR and Fourier Transform Infrared (FTIR) was in regular operation in room number-348 for the users. These have been shifted to CMCM area with the support of mechanical group and service engineers. Both the facilities have been shifted and re-installed and presently in regular operation for user's experiments. About 200 and 165 spectra have been taken using FTIR and UV-Vis-NIR facilities respectively for various users in the year 2022.

4.4.6.3 Thin film Deposition systems and high temperature furnaces

S. K. Kedia, F. Singh and V. V. Sivakumar

The sputtering system has been upgraded by replacing or repairing its various components such as temperature controller, substrate rotation, PID controller, vacuum gauge, thickness monitor and water, and air pipes. Sputtering system was dismantled and shifted to outside open area during renovation of the Laboratory (Room-205). The system has been assembled again in the designated space after lab renovation. A copper thin film of thickness 50 nm was deposited to test the system after assembling. The supports many users for preparing their thin films using RF sputtering. The evaporation system is capable of depositing the thin films from both thermal evaporation and electron beam induce evaporation techniques. The e-beam system has been dismantled and shifted to CMCM area of the Material Science Building. The machine has been assembled at the newly designated place in the CMCM area and leak tested. This system has machine had problems with the high vacuum gauge which was diagnosed and resolved. The work is in progress to deposit a few thin films to validate the re-installation. The synthesis of the films by sol-gel method has also been initiated after the renovation work and this is available for the regular use of the users including the in-house users. The high-temperature furnaces are in regular operations and are being used by the several users for calcination, annealing, and sintering of their samples in various temperature ranges.

4.5 RADIATION BIOLOGY

S. A. Khan and A. Tripathi

The ASPIRE [Automated Sample Positioning and Irradiation system for Radiation biology Experiments] system, which is used to conduct radiation biology studies with accelerated heavy ions, is housed in the dedicated radiation biology beamline at IUAC. Cells can be exposed to the desired dose of accelerated heavy ions in air at atmospheric pressure using this beamline. The setup offers a circular exposure area with a diameter of 4 cm in which the dose has a very good dosage homogeneity, within 2% standard variation. Two runs were taken in the beamline by Kalyani University group this year for irradiation with 85 MeV Carbon ion beam. A faulty germicidal ultraviolet fixture in the ASPIRE system was replaced before the beamtimes.

The computers attached to upright Fluorescence microscope (Zeiss Axioplan 2) and Perkin Elmer's Victor X5 Multimode Plate Reader were repaired this year. UV-Vis Spectrophotometer (Hitachi's U-3300) and Drop Shape Analyzer from Krüss GmbH (DSA100) have been shifted to Centre for Materials Characterization and Measurement (CMCM) in the LEIB building this year.

4.6 ATOMIC AND MOLECULAR PHYSICS

4.6.1 Status of vacuum chamber at 75° beam line in LEIBF

D. K. Swami and C.P. Safvan

Inter University Accelerator Centre, Aruna Asaf Ali Marg, New Delhi-110067, India.

X-ray spectroscopy experiments related to atomic physics, which operate at low ion beam energy, are conducted within a vacuum chamber located at the 75° beam line in LEIBF. To measure x-rays during these experiments, two silicon drift detectors (SDD) are utilized, with a resolution of approximately 140-150 eV at 5.9 keV. Additionally, two silicon surface barrier detectors are used to measure scattered and backscattered charged particles. The chamber has the capacity to hold 4-5 targets simultaneously, which can be moved linearly and angularly using a motion feed through and a rotatable axis-360° adjustable stage respectively, both mounted on the lid. A collimator (penetrable Faraday cup) is positioned at the entrance of the ion beam before the targets. The vacuum level within the chamber during experiments is between 10^{-6} - 10^{-7} mbar.

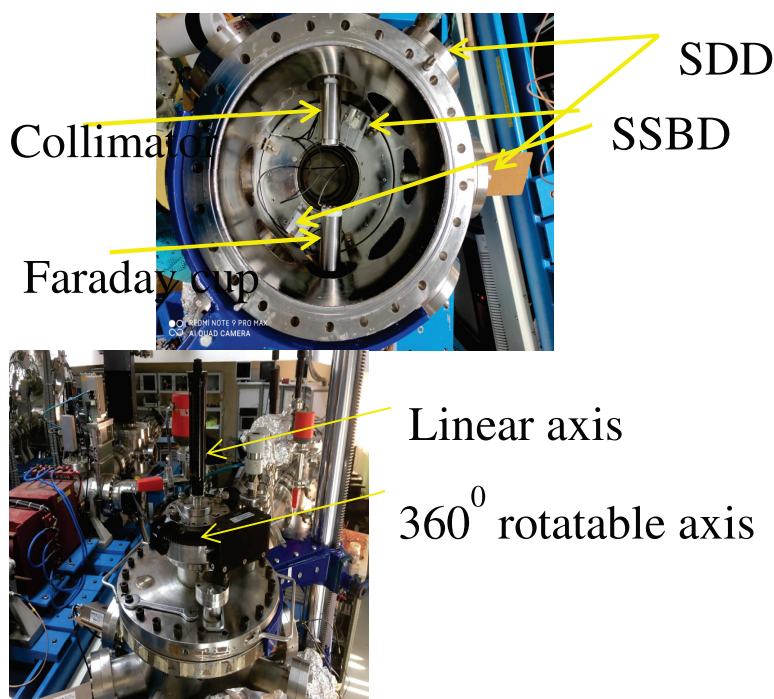


Fig. 1: Schematic of vacuum chamber at 75° beam line in LEIBF.

4.6.2 Status of general purpose atomic physics vacuum chamber (GPAC) at beam hall-II

D. K. Swami and C.P. Safvan

Inter University Accelerator Centre, Aruna Asaf Ali Marg, New Delhi-110067, India.

In the general purpose atomic physics vacuum chamber (GPAC) located at beam hall-II, experiments

involving the collision of highly charged ion beams with solids and subsequent x-ray spectroscopy are conducted. The experiments employ two silicon drift x-ray detectors (SDDs) that are positioned at different angles relative to the ion beam, and have an experimental resolution of approximately 140-150 eV at 5.9 keV. Additionally, two silicon surface barrier detectors are utilized to measure scattered and backscattered charged particles. Up to 10 targets can be employed simultaneously in the experiments. The vacuum level inside the chamber is maintained at 10^{-6} to 10^{-7} mbar during the experiments.

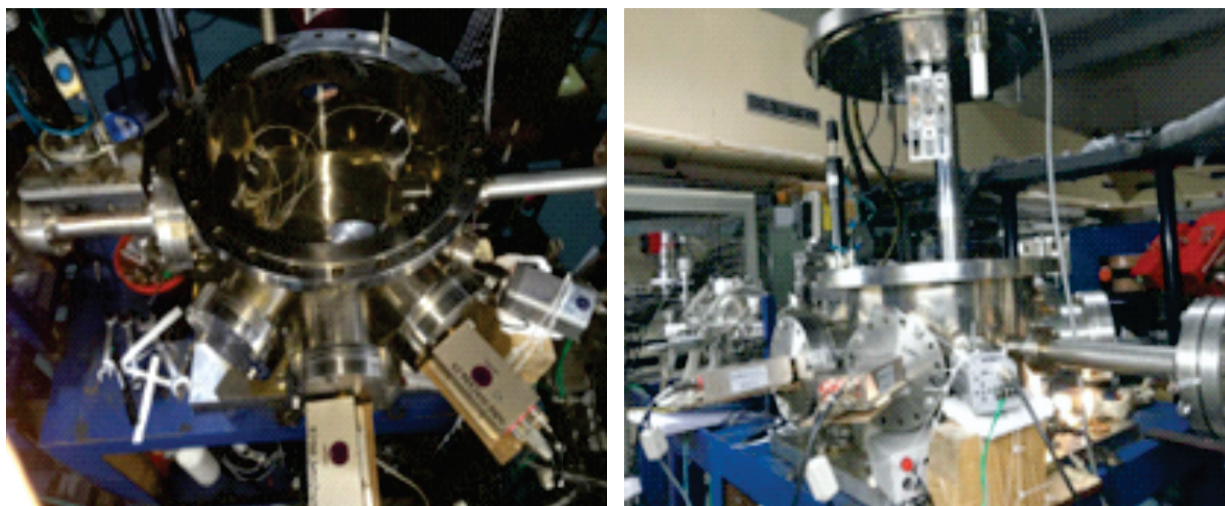


Fig.2: Schematic of GPAC in beam hall-II.

4.6.3 Status and modification of vacuum chamber at 105° beam line in LEIBF

Aditya Kumar, D. K. Swami and C.P. Safvan

Inter University Accelerator Centre, Aruna Asaf Ali Marg, New Delhi-110067, India.

A new setup for neutral beam formation with energy range of 50-350keV is established in 105° line of Low-energy ion beam facility at IUAC (fig.1). Such atom-molecule interactions have importance in the field of astrophysics for analysing interaction of solar winds with planetary atmospheres, also in medical science e.g. radiotherapy for improving proton dosimetry in treatment planning. New chamber, consisting of carbon foil (20nm thickness) for neutral beam formation, have installed with alignment and tested for vacuum. For extraction of neutral particles out of charged ones, one newly designed electrostatic separator also installed in beam line. Inside big chamber, one newly designed collimator, and detector for neutrals is mounted. Alignment of all the setup/instrument along with power connection have done successfully. Vacuum of 10^{-7} - 10^{-8} torr also achieved and this new setup is ready for test run.

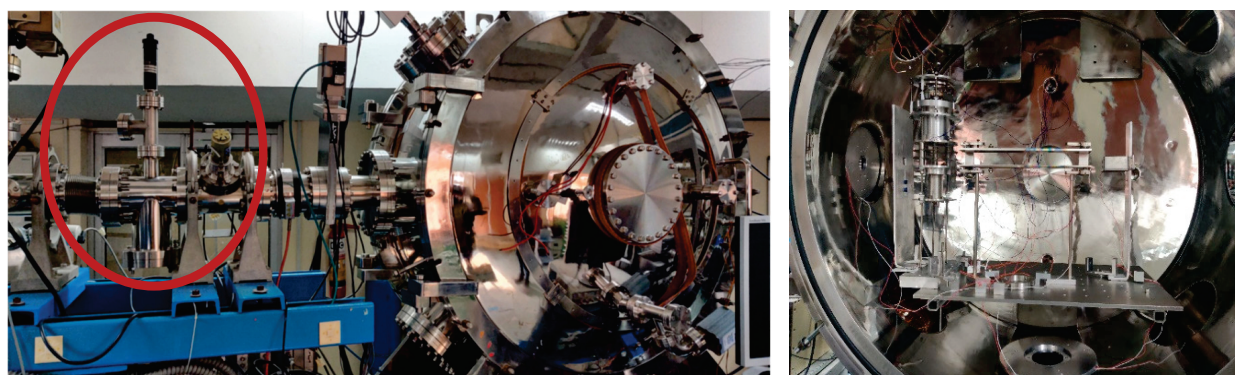


Fig.3. Chamber for neutral formation in 105° line of L.E.I.B.F.

4.6.4 Status of Ion trap

Deepak Chinwal, Sugam Kumar, D. K. Swami and C.P. Safvan

Inter University Accelerator Centre, Aruna Asaf Ali Marg, New Delhi-110067, India. At IUAC, work is underway to develop an ion trap, and several preliminary tests are being conducted. These tests involve assessing the vacuum conditions necessary for the experiment and ensuring that each component is compatible with the system. Additionally, the electron gun's performance in ionizing gas is being evaluated, and the Channeltron detector has been tested in conjunction with the electron gun. The storage time of ion

depends on the vacuum. Therefore, ultra-high vacuum 10^{-7} - 10^{-8} mbar is maintained inside the chamber. The test was conducted to now the optimal condition at which gun can be operated. Electron gun was functioning properly. The assembly of experimental setup has been completed as shown in figure 4. A preliminary test will be performed with hydrogen gas. This will help us in analysing the optimal condition for ion trapping.



Fig. 4: Experimental setup of Ion trap